Quantitative analysis of the binding affinity of poly(ADP-ribose) to specific binding proteins as a function of chain length

Jörg Fahrer[1], Ramon Kranaster[2], Matthias Altmeyer[1], Andreas Marx[2] and Alexander Bürkle[1],*

[1]Department of Biology, Molecular Toxicology Group and [2]Department of Chemistry, University of Konstanz, Universitätsstrasse 10, D-78457 Konstanz, Germany

ABSTRACT

Poly(ADP-ribose) (PAR) is synthesized by poly(ADP-ribose) polymerases in response to genotoxic stress and interacts non-covalently with DNA damage checkpoint and repair proteins. Here, we present a variety of techniques to analyze this interaction in terms of selectivity and affinity. *In vitro* synthesized PAR was end-labeled using a carbonyl-reactive biotin analog. Binding of HPLC-fractionated PAR chains to the tumor suppressor protein p53 and to the nucleotide excision repair protein XPA was assessed using a novel electrophoretic mobility shift assay (EMSA). Long ADP-ribose chains (55-mer) promoted the formation of three specific complexes with p53. Short PAR chains (16-mer) were also able to bind p53, yet forming only one defined complex. In contrast, XPA did not interact with short polymer, but produced a single complex with long PAR chains (55-mer). In addition, we performed surface plasmon resonance with immobilized PAR chains, which allowed establishing binding constants and confirmed the results obtained by EMSA. Taken together, we developed several new protocols permitting the quantitative characterization of PAR–protein binding. Furthermore, we demonstrated that the affinity of the non-covalent PAR interactions with specific binding proteins (XPA, p53) can be very high (nanomolar range) and depends both on the PAR chain length and on the binding protein.

INTRODUCTION

The superfamily of poly(ADP-ribose) polymerases (PARPs) comprises over a dozen proteins, which have been identified in most eukaryotic organisms but are absent in yeast and prokaryotes (1). PARP-1 is the best-characterized member of this family and is activated via binding to single- or double-strand breaks in DNA to catalyze the transfer of ADP-ribose moieties from NAD^+ on acceptor proteins, thus producing protein-coupled PAR chains (2), which can be degraded by poly(ADP-ribose) glycohydrolase (PARG) in an endo- and exo-glycosidic manner (3). Very recently two novel isoforms of PARG have been identified, which possess mitochondrial targeting sequences and may participate in the signaling of PAR from the nucleus to mitochondria (4). PARP-1 represents the predominant target ('acceptor') protein undergoing this covalent modification, but other nuclear proteins including p53, NF-κB, CSB and histones are poly(ADP-ribosyl)ated as well (5–9). PARP-1 is functionally associated with DNA repair and contributes to the maintenance of genomic stability thereby counteracting cancer formation (10–15). PAR is a nucleic acid analog and consists of a heterogeneous mixture of linear and branched chains ranging from 2 up to 200 ADP-ribose units *in vivo* (16). Owing to the ribose–phosphate–phosphate–ribose backbone PAR has a higher negative charge density as compared to DNA and was suggested to exhibit a helical conformation (17). It was proposed that non-covalent interactions with other molecules, for example with constitutive components of chromatin, play a crucial role in polymer function (18). It is conceivable that non-covalent interactions with PAR depend on chain length and branching complexity (19). Several years ago Pleschke and colleagues (20) identified a PAR-binding motif in a variety of proteins involved in DNA damage checkpoint and repair. Non-covalent interaction is mediated by a conserved consensus sequence, which is frequently located within functional protein domains. Binding was proposed to regulate DNA–protein and protein–protein interactions as well as protein degradation. Non-covalent binding of PAR to p53 dramatically reduces its DNA-binding activity

*To whom correspondence should be addressed. Tel: +49 7531 884035; Fax: +49 7531 884033; Email: alexander.buerkle@uni konstanz.de

in a concentration-dependent manner (21). XRCC1, another protein harboring this consensus motif, specifically interacts with poly(ADP-ribosyl)ated PARP-1 via the PAR chains that are covalently attached to PARP-1. Thus XRCC1 is recruited to the site of DNA damage stimulating base excision repair (22,23). Topoisomerase 1, which is also involved in genomic stability, possesses three PAR-binding sites overlapping with structurally and functionally important domains (24). PAR was shown to reactivate stalled topoisomerase 1 and to promote DNA strand break resealing. Very recently a physical and functional interplay of protein kinase Ataxia telangiectasia mutated (ATM), which is involved in the early DNA damage response, and PAR has been established (25). Moreover, PAR was demonstrated to associate with mitotic spindles and to be required for spindle function in *Xenopus laevis* egg extracts (26). The increasing number of biological processes, in which PAR is involved, highlights the importance of this complex biopolymer (27). Binding of PAR to proteins is not only highly specific but also very stable, e.g. histone H1–PAR complexes resist phenol partitioning, high-salt washes and detergents (28). So far, however, virtually nothing is known concerning the selectivity and affinity of this interaction. Merely histones were characterized with regard to chain length using an *in vitro* phenol-partitioning assay, which revealed a preferential binding of histones to long and branched ADP-ribose chains (28,29).

We established several novel methods to assess the non-covalent interaction between PAR and specific binding proteins as a function of PAR chain length. In particular, we end-labeled ADP-ribose chains with a biotin moiety and subsequently fractionated PAR by high-resolution anion exchange HPLC to obtain ADP-ribose chains of defined length. In order to quantify the binding affinities to selected proteins (p53, XPA), we developed an electrophoretic mobility shift assay (EMSA) and used surface plasmon resonance (SPR) to determine the binding kinetics. We demonstrate for the first time that non-covalent PAR–protein interactions exhibit extraordinary high affinities (nanomolar range) and display a hitherto unknown selectivity with regard to both chain length and the binding protein.

MATERIALS AND METHODS

Material

Mouse monoclonal antibody 10H was immuno-purified on a protein A column (Sigma) from culture supernatant of 10H hybridoma cells (30). Q Sepharose FastFlow was from Amersham Biosciences and Ni-NTA Superflow was purchased from Qiagen. TCA, EDTA and 40% acrylamide solution (19:1) was from Roth. NaCl and ethanol were obtained from Riedel-de Häen. The octameric oligonucleotide GGAATTCC was purchased from Invitrogen. All other chemicals were obtained from Sigma-Aldrich.

Protein expression and purification

Recombinant PARP-1 was overexpressed in Sf9 cells using the baculovirus system and purified as described (31) except that the oligo-dT/poly-A cellulose step was replaced by a dsDNA-cellulose (Sigma) column chromatography. p53 was overexpressed in High-Five insect cells and isolated by anion exchange and DNA cellulose affinity chromatography (32,33). The cDNA encoding for XPA was cloned into baculovirus expression vector pVL 1392 (BD Biosciences), expressed as His-tagged fusion protein and purified by Ni-NTA chromatography followed by DNA cellulose affinity chromatography (34,35).

Synthesis and purification of PAR

According to Kiehlbauch *et al.* (19), PAR was synthesized with some modifications. Briefly, PAR was synthesized in a 20 ml incubation mixture comprising 100 mM Tris–HCl pH 7.8, 10 mM $MgCl_2$, 1 mM NAD^+, 10 mM DTT, 60 µg/ml histone H1, 60 µg/ml histone type IIa, 50 µg/ml octameric 'activator' oligonucleotide GGAATTCC and 150 nM human PARP-1. The reaction was stopped after 15 min by addition of 20 ml ice-cold 20% TCA. Following precipitation the pellet was washed with ice-cold 99.8% ethanol. Polymer was detached using 0.5 M KOH/50 mM EDTA and purified as described (36). After extraction with phenol–chloroform–isoamyl alcohol PAR was precipitated with ethanol overnight. Following centrifugation PAR was air-dried and stored at −20°C

Biotinylation of ADP-ribose chains

Typically 150 nmol of purified PAR synthesized *in vitro* were incubated under reductive amination conditions in sodium acetate buffer pH 5.5 containing 4 mM biocytin hydrazide (Pierce) in a total volume of 500 µl for 8 h at room temperature. Following dialysis overnight polymer was precipitated with ethanol and concentrations were determined using UV absorbance at 258 nm (37). Successful labeling was confirmed by 20% native PAGE and subsequent semi-dry blot onto a nylon membrane (Amersham Biosciences). After blocking with 2% bovine serum albumin (BSA) in Tris-buffered saline–Tween 20 (TBS-T) solution biotinylated PAR was detected by streptavidin–POD (Amersham Biosciences). Bands were visualized by chemiluminescence imaging using a FujiLAS 1000.

HPLC fractionation of polymers and characterization on sequencing gels

Polymer fractionation was performed using a Shimadzu LC-8A HPLC system equipped with a semi-preparative DNA Pac PA100 column (DIONEX). Five micromole of purified, biotinylated PAR were applied to the column and polymers were eluted using a multistep NaCl gradient in 25 mM Tris–HCl pH 9.0 modified from Kiehlbauch *et al.* (19). Fractions were collected manually according to UV absorbance at 258 nm. Separated biotin-labeled PAR was precipitated with ethanol, dissolved in 500 µl water and stored at −20°C. Subsequently, ADP-ribose polymers were characterized on modified sequencing gels (18). Typically 50 pmol of the respective fraction were subjected to electrophoresis and separated polymers were visualized using GELCODE Color silver stain (Pierce) as described (36).

Binding of immobilized proteins to PAR

Typically 15 pmol of recombinant protein was vacuum aspirated onto nitrocellulose membranes (Amersham Biociences) using a slot-blot manifold (Schleicher & Schuell). The membranes were cut into appropriate pieces and these were incubated with 500 pmol of the respective ADP-ribose fraction in 5 ml TBS-T. After three washing steps with TBS-T containing 1 M NaCl, membranes were blocked with 5% (w/v) skim milk powder in TBS-T, bound polymers were detected using 10H antibody and secondary peroxidase-conjugated anti-mouse IgG (DakoCytomation). Bands were visualized in the FujiLAS1000 device using enhanced chemiluminescence. Evaluation of blots was performed with AIDA software (Raytest).

Affinity purification of biotinylated PAR

Prior to gel shift experiments end-biotinylated fractionated PAR was affinity-purified using SoftLink^{TM} Soft Release Avidin Resin (Promega) as described in the user manual. Briefly, biotinylated polymer was diluted in bind and wash (BW) buffer containing 50 mM Tris–HCl pH 8.0, 50 mM NaCl to 2 ml and applied to the resin. The flowthrough was collected and loaded once again. Subsequently, the column was washed with 6 ml BW buffer and bound biotinylated PAR chains were gently eluted in 1 ml steps using 5 mM D(+)-biotin. The purification process was monitored by native 20% PAGE and detection was performed using streptavidin–POD and enhanced chemiluminescence.

Eluted biotinylated PAR was pooled and dialyzed against MilliQ water overnight. Thereafter samples were lyophilized using a Speed Vac and dissolved in 100 μl MilliQ water. Concentration of affinity-purified PAR was determined by native PAGE using a 49-mer oligonucleotide (Invitrogen) as standard.

PAR electrophoretic mobility shift assay

The protein of interest was incubated in an appropriate volume of 10 mM Tris–HCl pH 7.4, 1 mM EDTA for 10 min at 25°C. Affinity-purified biotinylated PAR of defined chain length (250 fmol of 16-mer and 125 fmol of 55-mer, respectively) was added and complex formation was allowed for 20 min at 25°C to reach equilibrium. Subsequently the reaction mixture was supplemented with 10× loading dye resulting in a final volume of 25 μl. The samples were electrophoresed through 5% native polyacrylamide gels for 2.5 h at 160 V to separate free and bound ADP-ribose polymer. Thereafter, samples were transferred to a nylon membrane via semi-dry blotting. Then the membrane was blocked with 2% BSA in TBS-T and biotinylated ADP-ribose chains were detected with streptavidin–POD. Blots were visualized using a FujiLAS 1000 chemiluminescene imager and quantification was performed using AIDA Software.

Surface plasmon resonance

All SPR binding sensorgrams were obtained with Biacore T100 and SA sensor chips (GE Healthcare).

Biotinylated PAR (14-mer or 63-mer) was immobilized on a streptavidin-coated SA sensor chip. Briefly, a 5 nM solution of the respective PAR chain in PBS buffer pH 7.4 was injected over the flow cell to obtain a response level of 8–12 RU (14-mer) and 3–5 RU (63-mer), respectively. A reference cell without immobilized ligands was used to subtract buffer refractive effects and as a control for unspecific binding. Furthermore, specificity of sensor surface was checked using monoclonal antibody 10H as positive control and BSA as negative control. The following concentrations of 10H were injected: 0.01, 0.05, 0.1, 1.0, 2.0, 2× 5.0 and 10 nM at a flow rate of 60 μl/min, 120 s contact time, 600 s dissociation time. This was followed by a first (30 s contact time, 2 M NaCl + 0.1% SDS) and a second regeneration step (60 s contact time, 2 M NaCl + 0.1% SDS). The following concentrations of XPA were injected: 5.0, 10, 50, 2× 100, 200, 300, 400 and 500 nM. Flow rate was 50 μl/min, 70 s contact time, 600 s dissociation time. This was followed by a first (60 s contact time, 6 M guanidine HCl) and a second regeneration step (90 s contact time, 2 M NaCl + 0.1% SDS). For kinetic titration a 2-fold dilution series of p53 was injected as follows: 1000, 500, 250, 125 and 62.5 nM (for PAR 14-mer); 400, 200, 100, 50 and 25 nM (for PAR 63-mer). Data evaluation was carried out using Biacore T100 Evaluation 1.1.1. which allows the fitting of experimental data with implemented kinetic models. In the case of kinetic titration, data were evaluated with BIAevaluation software 4.1.

Statistical analysis

EMSA data are displayed as means + SEM. Each EMSA experiment, done in triplicates, was performed at least twice. The data obtained were analyzed using GraphPad Prism 4 software, and K_D values were calculated by using a sigmoidal dose–response curve with variable slope. Curves were fitted using non-linear regression.

RESULTS

Terminal biotinylation of PAR

A number of methods to study PAR function have been established, but their power is often limited due to the large heterogeneity of PAR. Several efforts have been made to fractionate this complex polymer according to chain length (18,19,38). Despite successful small-scale fractionation of PAR into defined size classes no study has been performed so far to investigate the impact of chain length on PAR–protein interactions. Major obstacles were the amount of ADP-ribose polymers required and the lack of tools to detect interactions without using PAR-specific antibodies.

We therefore set out to develop a new method for specific end-labeling of PAR chains. Purified PAR synthesized *in vitro* was coupled to biotin via a carbonyl-reactive biotin analog (biocytin hydrazide) (Figure 1A). This molecule attacks the reducing ribose terminus of the polymer chain, forming a stable bond under reductive amination conditions. The labeling reaction was time dependent as monitored by semi-dry blotting and reached
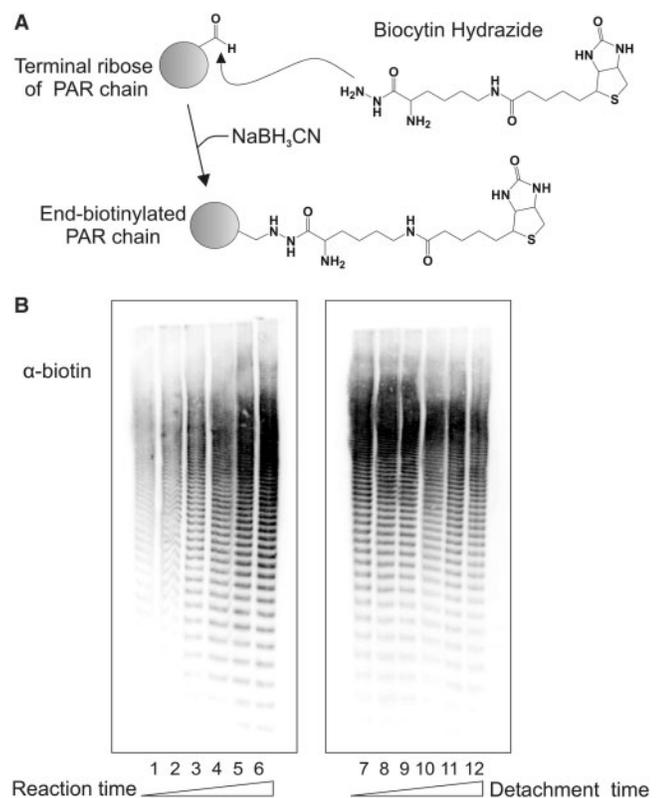
Figure 1. Terminal labeling of PAR chains. (**A**) Structure of the carbonyl reactive linker biocytin hydrazide. (**B**) Biotinylation of PAR chains is time dependent. End labeled PAR samples were subjected to native PAGE and transferred to a nylon membrane. Detection was performed using streptavidin POD. The panel on the left displays the time dependency of the labeling reaction (lane 1 6; 0.25, 0.5, 1, 2, 4 and 8 h). The panel on the right shows the impact of KOH detachment time during PAR isolation on subsequent biotin labeling (lane 7 12; 5, 15, 30, 45, 60 and 120 min).

Figure 2. Interaction of fractionated PAR and immobilized proteins. (**A**) Recombinant purified p53 was vacuum aspirated onto a nitrocellu lose membrane using a slot blot manifold (15 pmol/slot). The mem brane was cut into slices and incubated with PAR fractions comprising distinct polymer size classes. After several washing steps with high stringency to disrupt unspecific protein polymer interactions, bound PAR was detected by monoclonal antibody 10H followed by incuba tion with goat α mouse HRP and peroxidase reaction. A representative slot blot with triplicate determinations is shown. (**B**) Comparison of PAR binding with regard to chain length between XPA and p53. Signal intensity is indicated in arbitrary units. The bars represent mean + SEM of triplicates. Note the superior binding capacity of XPA for 20 49 mers, compared to p53.

a maximum after 8 h (Figure 1B, left panel). Interestingly, even very short ADP-ribose chains were efficiently biotinylated, yet the pattern of biotinylated PAR did reflect the distribution of synthesized ADP-ribose poly mers. In addition, we observed that the extent of labeling depends on the incubation period used for detachment of the polymer from the acceptor protein during PAR purification (Figure 1B, right panel). With increasing time of incubation of the protein-coupled polymer under strong alkaline conditions the yield of the terminal biotinylation reaction decreased. This may be attributable to the elimination of the terminal ribose moiety catalyzed by strong bases (19). The overall yield of biotinylated PAR was 10–20% as estimated by affinity chromatogra phy/UV absorbance (data not shown).

In conclusion, we established specific biotin end-labeling of PAR, which enables novel biochemical analyses of this biopolymer, e.g. affinity studies, employ ing streptavidin–biotin chemistry.

Binding of PAR to immobilized proteins is influenced by chain length

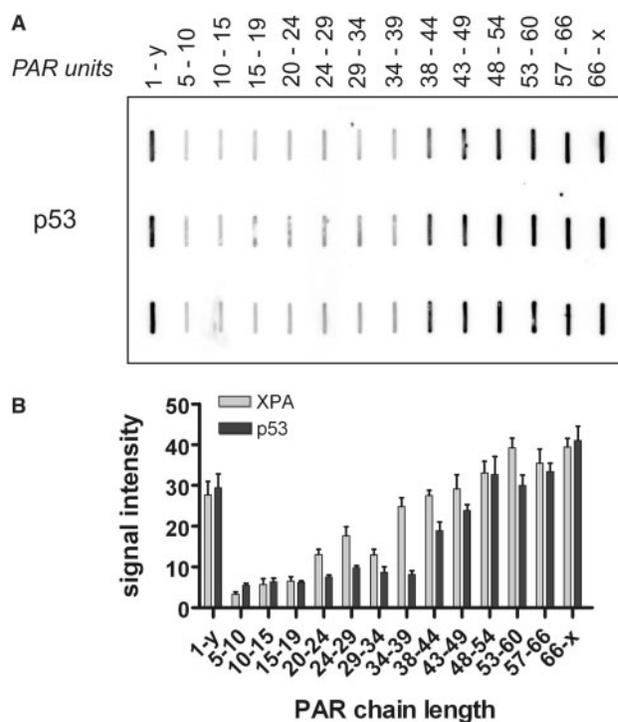Terminally biotinylated PAR was fractionated according to chain length using an anion exchange HPLC protocol

as described by Kiehlbauch *et al*. (19), with modifications. The semi-preparative column we used permits the separa tion of 5–10 µmol PAR in contrast to previous analytical columns with a limit of only 100 nmol PAR (19). The fractions of biotinylated polymers were analyzed on modi fied sequencing gels to assess chain length and purity. Silver staining showed the successful separation of ADP-ribose polymers of defined size class ranging from 3 up to 70 ADP-ribose units (data not shown).

To assess the non-covalent binding of fractionated PAR chains to proteins, a classical approach was chosen. Equal amounts of each purified protein were immobilized on a nitrocellulose membrane and bound ADP-ribose chains were detected using the monoclonal PAR antibody 10H. The human tumor suppressor protein p53 was previously shown to interact in a non-covalent fashion with PAR and harbors three potential PAR-binding sites (20). Since the binding of PAR to p53 influences its DNA-binding acti vity we asked whether there was specificity for a certain polymer size class. Surprisingly, ADP-ribose chains ranging from 5 up to 39 units bound rather poorly to p53 (Figure 2A) whereas longer PAR chains displayed a higher affinity. Furthermore, the binding of separated
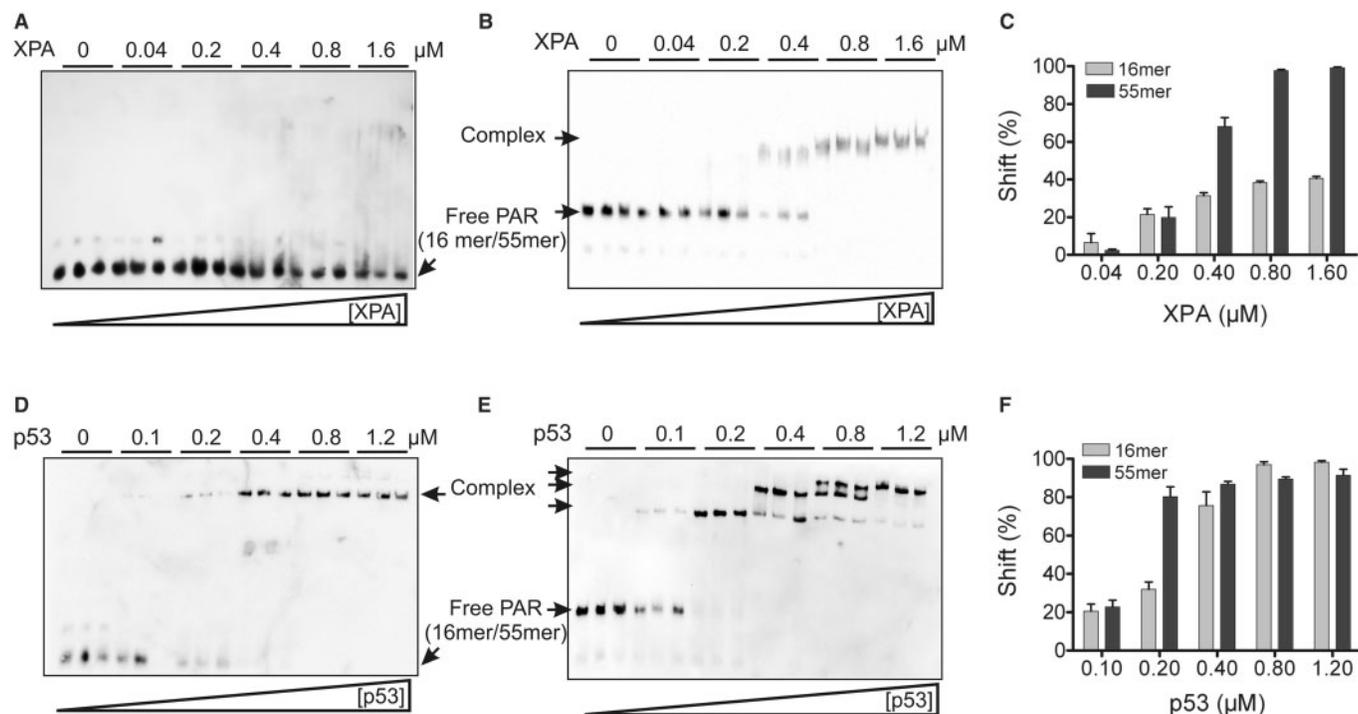
Figure 3. Interaction of fractionated PAR and binding proteins in solution as assessed by EMSA. Briefly, biotinylated PAR of a defined size was incubated with binding proteins and subjected to native PAGE followed by semi dry blotting. Bound and free ADP ribose chains were detected using streptavidin POD. (**A**) Binding of short PAR chains (16 mer) to XPA. (**B**) Binding of long PAR chains (55 mer) to XPA. (**C**) Quantitative evaluation of XPA gel shifts. Shift (%) was calculated as follows: signal intensity complexed PAR/(complexed + free PAR). Data are expressed as mean + SEM of triplicates from two independent experiments. (**D**) Binding of short PAR chains (16 mer) to p53. (**E**) Binding of long PAR chains (55 mer) to p53. (**F**) Evaluation of p53 gel shifts as described in (C).

PAR chains to immobilized human XPA was monitored. Short chains of up to 20 ADP-ribose moieties displayed weak affinity for XPA similar to the experiments performed with p53 (Figure 2B). Interestingly, PAR chains of 20–40 units showed higher affinity to XPA, compared to p53. PAR with more than 40 ADP-ribose units bound very tightly to XPA, comparable to p53.

Taken together, these experiments indicated a pivotal role of PAR chain length for regulating PAR–protein interactions.

Proteins display differential binding for PAR depending on chain length

To further analyze the non-covalent interaction of PAR and binding proteins as a function of chain length, a PAR EMSA was established. Increasing concentrations of recombinant XPA were incubated with fixed amounts of avidin affinity-purified short ADP-ribose chains (16-mer) and samples were subjected to native PAGE. Free as well as bound PAR polymer was detected via the terminal biotin-label using streptavidin–POD (Figure 3A). No specific interaction of XPA with short ADP-ribose chains was observed. At high XPA concentrations apparently some binding of PAR did occur, however without formation of a defined complex. Using long PAR chains (55-mer) XPA produced a complex in a concentration-dependent manner (Figure 3B). A concentration of $0.6\,\mu M$

XPA was sufficient for complete binding of the available free polymer. Densitometric evaluation of the blots is depicted in Figure 3C, displaying the significant difference in PAR binding. In contrast, p53 promoted specific complex formation with short-PAR chains starting at $0.1\,\mu M$ of p53 (Figure 3D). PAR was almost completely bound at $0.8\,\mu M$ p53, as was detected by the formation of one discrete complex appearing at the top of the gel. The same set of experiments was repeated using long ADP-ribose molecules with an average chain length of 55 units (Figure 3E). Binding was detected already at or above $0.1\,\mu M$ p53 and was nearly complete at $0.2\,\mu M$ demonstrating the higher affinity of p53 for long chains. Strikingly, we observed that p53 was able to form three distinct specific complexes with long-PAR chains at higher concentrations. Blots were quantified and summarized clearly indicating the different affinities of p53 with regard to chain length (Figure 3F). Since all measurements were made in equilibrium, the EMSA results allowed the calculation of K_D values representing the affinities of the respective proteins to the isolated PAR chains. The K_D values we determined were all in the nanomolar range, demonstrating the high affinity of this non-covalent interaction (Table 1; Supplementary Table S1). In addition, there exists a binding specificity with regard to chain length as XPA was not able to form a specific complex with short ADP-ribose molecules in solution.

Table 1. Equilibrium constants derived from EMSA and SPR studies on the binding of proteins to fractionated PAR

		16/14 mer PAR K_D [M]	55/63 mer PAR K_D [M]
EMSA	XPA	NB	$3.2 \times 10^{-7} \pm 7.7 \times 10^{-9}$
SPR	XPA[a]	NB	$6.5 \times 10^{-9} \pm 1.3 \times 10^{-10}$
EMSA	p53	$2.5 \times 10^{-7} \pm 3.8 \times 10^{-8}$	$1.3 \times 10^{-7} \pm 4.2 \times 10^{-9}$
SPR	p53[b]	$3.4 \times 10^{-9} \pm 1.0 \times 10^{-11}$	NM
SPR	10H[c]	$2.8 \times 10^{-9\ [d]} \pm 1.2 \times 10^{-12}$	$3.5 \times 10^{-10\ [d]} \pm 3.0 \times 10^{-12}$

NB indicates no binding observed with up to 500 nM analyte.
NM indicates no model found for describing such complex binding.
[a]Original data fitted with conformational change model.
[b]Original data deriving from kinetic titration (40) fitted 1:1.
[c]Original data fitted with bivalent binding model.
[d]Equilibrium dissociation constant obtained from (k_{d1}/k_{a1}).

Surface plasmon resonance analyses of PAR–protein interaction

To obtain more quantitative information we performed SPR real-time binding studies. SPR systems are optical biosensors that allow probe-free quantitative analysis of biomolecular interactions (39). Two different biotinylated PAR chains (14-mer and 63-mer) were immobilized on streptavidin-coated sensor chips. Successful immobilization was checked by using monoclonal PAR antibody 10H. Specificity of the sensor surface was tested using BSA, which did not interact with the immobilized PAR at all (data not shown). Regeneration conditions were established successfully except for p53, which was therefore analyzed using kinetic titrations (40).

Antibody 10H showed very high affinity and fast association to both short and long PAR chains. Curves were fitted with a bivalent binding model (Figure 4A and B). The binding equilibrium of the first binding event was calculated to be 2.8 nM for the short and 0.35 nM for the long PAR chain (Table 1; Supplementary Table S1).

Using XPA at up to 500 nM, no significant binding was observed with the short PAR oligomer whereas XPA displayed high affinity for long PAR chains (63-mer) with a K_D value of 6.5 nM (Table 1; Supplementary Table S1) and thus confirming the results obtained by EMSA (Figure 4C and D). Best fits of the resulting data were obtained using a conformational change binding model based on the assumption that first a weakly bound binding state between the PAR chain and XPA is formed and a second tighter binding state is reached after a conformational change (41). In contrast, p53 displayed strong binding to both short and long PAR chains (Figure 4E and F). Especially for long PAR chains binding behavior is difficult to describe as p53 forms up to three PAR–protein complexes as shown in EMSA experiments (Figure 3E). Using short PAR chains (14-mer) satisfactory fitting of the data was achieved with the Langmuir (1:1)-binding model (40) providing a K_D value of 3.4 nM (Table 1; Supplementary Table S1). These data are in line with the EMSA experiments, showing that p53 produces a single complex with short polymer.

Furthermore, we were able to estimate the stoichiometry of the PAR–protein complexes, using the observed maximum binding capacity R_{max} of the respective protein, the molecular weight ratio of the different analytes and ligands and the immobilized amount of PAR (Supplementary Table S1) (42). Disregarding the possibility of protein multimerization, antibody 10H displayed the highest binding stoichiometry with up to 21 molecules per 63-mer, implicating that one antibody molecule requires only 3–4 ADP-ribose units for efficient binding. p53 required 4–6 ADP-ribose units for efficient binding to long PAR. XPA showed a stoichiometry of four protein molecules per 63-mer chain and therefore requires ~16 ADP-ribose units for binding. It should be mentioned that these values are only estimates due to the low amount of immobilized PAR (see Material and Methods section) and neglected protein oligomerization before or after binding to the surface, which is already known to occur in the case of p53 (43).

DISCUSSION

We have shown that efficient terminal biotinylation of ADP-ribose chains is feasible and provides a novel, versatile tool to study the non-covalent PAR–protein interaction in liquid as well as in solid phase experiments. Previous approaches have explored photoreactive biotin analogs or biotinylated NAD^+ to label PAR chains, leading to the unselective incorporation of several biotin moieties (44,45). Other studies used ^{32}P-NAD^+ to label PAR radioactively (18,19), which is however not suited for large-scale preparations and does not offer the advantages of an affinity tag, e.g. biotin. In contrast, terminal modification of PAR with biotin allowed specific immobilization of separated ADP-ribose chains on streptavidin-coated surfaces and permitted the use in other applications such as EMSA.

Recent protocols have used analytical anion exchange HPLC and MonoQ anion exchange FPLC to size-fractionate up to 100 nmol PAR (19,36). Unlike these methods, the established semi-preparative HPLC allowed the fractionation of up to 10 μmol of PAR, which is equivalent to 100 runs using analytical HPLC.

By means of a slot blot assay we showed that the chain length of PAR has a strong effect on its interaction with p53 and XPA. p53 displayed lower affinity for ADP-ribose chains of up to 39 units, but strongly bound long-PAR chains. Binding of separated ADP-ribose chains to XPA is also influenced by polymer size and increased with growing chain length.

The immobilization of proteins on a membrane results in an enhanced rigidity of the protein and is likely to alter protein conformation, which may affect polymer binding. To overcome such possible limitations, we developed a novel PAR-EMSA using end-biotinylated, fractionated PAR chains. We observed that p53 could interact with both short (16-mer) and long chains (55-mer), promoting the formation of specific complexes. Interestingly, p53 formed three distinct complexes with long PAR chains whereas only one complex was produced with short chains at high p53 concentrations. This suggests that long PAR chains induce higher molecular weight complexes
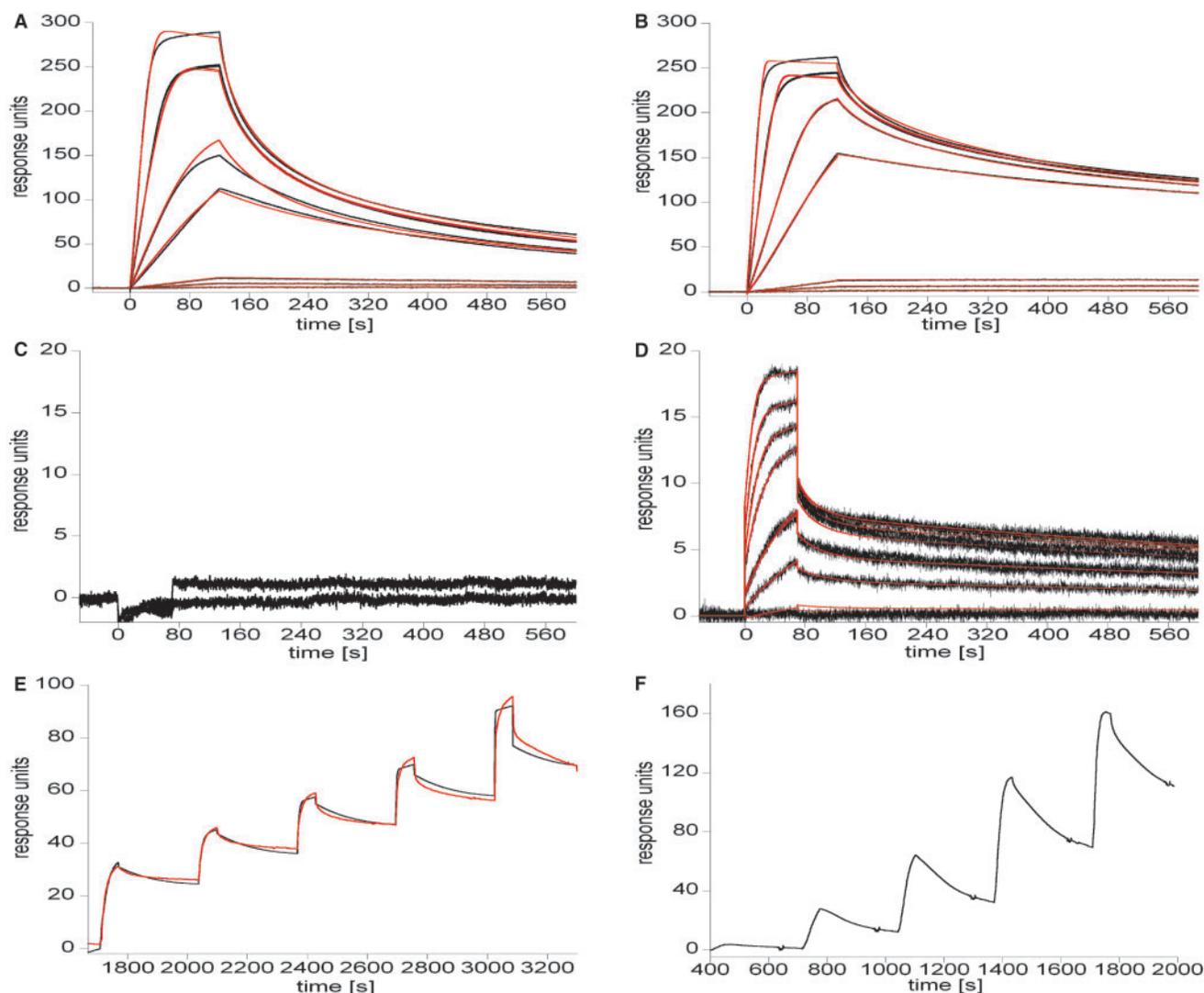
Figure 4. SPR real time binding studies with PAR 14 mer (**A**, **C** and **E**) and 63 mer (**B**, **D** and **F**). Experimental data are depicted in black and fitted curves in red. (A) Sensorgram of binding of antibody 10H (various concentrations from 0.01 to 10 nM) to PAR 14 mer using bivalent binding model for data evaluation. (B) Sensorgram for antibody 10H (various concentrations from 0.01 to 10 nM) binding to PAR 63 mer and bivalent binding model for data evaluation. (C) Sensorgram for XPA (50 and 100 nM) injected over immobilized PAR 14 mer. Even at 500 nM XPA no binding was observed. (D) Sensorgram for XPA binding to PAR 63 mer, with data fitted using a conformational change binding model. (E) Kinetic titration sensorgram for p53 binding to PAR 14 mer using a 1:1 binding model for data fitting. (F) Kinetic titration sensorgram for p53 binding to PAR 63 mer. Due to complex binding behavior (up to three different complexes) no satisfactory data fit was possible.

of p53, possibly by bridging two or more p53 molecules. Another possibility is that p53 complexes are formed in solution due to the increasing p53 concentration, but in the same experimental setup using short PAR chains such higher order structures of p53 were not observed (Figure 3D). Additionally, p53 harbors three PAR-binding sites and each of them may form independent complexes depending on their respective affinities. This hypothesis is confirmed by SPR measurements of single p53 injections which are best fitted with a binding model assuming three independent binding domains and three different resulting complexes (data not shown). Two PAR-binding sites are located in the DNA-binding domain and another motif resides in the tetramerization domain (20). Oligomerization of p53 is known to be pivotal for DNA

binding and its affinity to its DNA consensus sequence (43). The high affinity of short and, even more so, of long PAR chains to p53 therefore support the finding that PAR dramatically reduces the sequence-specific and the unspecific DNA binding of p53 (21).

Additionally, the binding properties of the nucleotide excision repair (NER) protein XPA to PAR of defined chain length were assessed using EMSA and SPR technique. Unlike p53, XPA did not form a specific complex with short chains, but produced a complex with long ADP-ribose molecules (55-mer) in a concentration-dependent manner (Figure 3B). XPA showed a comparable affinity for long-PAR chains as p53, being in the nanomolar range. These results were confirmed using the SPR approach, which showed no interaction of XPA

with short ADP-ribose chains (14-mer). The calculated stoichiometry for the non-covalent PAR–XPA interaction indicated that ∼16 ADP-ribose units are necessary for binding. Furthermore, SPR demonstrated that XPA binds to immobilized long PAR chains (63-mer) with considerably high affinity, i.e. in the low nanomolar range (Figure 4D). K_D values derived from SPR measurements are ∼50-fold lower compared to EMSA analysis, which is a general phenomenon already been described in the literature (46). XPA is involved in damage verification during NER and anchors structure-specific endonucleases to the damaged site (47). Additionally, it can interact with the transcription factor TFIIH. A PAR-binding site has been identified in the C-terminal part of XPA overlapping with the TFIIH interaction domain (20). It is conceivable that non-covalent interaction with long PAR molecules reduces DNA binding of XPA and/or may interfere with TFIIH protein interaction. Therefore, PAR might play a role in regulating XPA activity during NER.

In the present study, we established PAR chain length as a crucial determinant for specific, high-affinity non-covalent interactions with proteins. Depending upon the cellular situation, e.g. the presence of mild genotoxic stress, PARPs might catalyze the synthesis of PAR chains varying in chain length and branching complexity in order to recruit specific proteins and modulate their functions. A growing body of evidence shows that the activity of PARP-1 is tightly regulated by phosphorylation and protein interactions (48–51). For example, it was recently reported that NMN adenylyl transferase 1 (NMNAT-1), an enzyme involved in NAD^+ biosynthesis, functionally associates with PARP-1 thereby stimulating PARP-1 activity (51). Such interaction is likely to change the pattern of synthesized PAR with regard to chain length and branching. Strikingly, overexpression of NMNAT-1 resulted in increased translocation of apoptosis-inducing factor (AIF) upon oxidative stress, which fits with the previous observations that in response to severe genotoxic stress PAR formation is a death signal and triggers the release of AIF leading to caspase-independent cell death (52–54). Interestingly, it was observed that it was especially long-chain PAR with more than 60 ADP-ribose residues that induced high rates of cell death, whereas short polymers with 16 ADP-ribose units had only little effect on cell survival. This underscores the importance of PAR as a signaling molecule and emphasizes the pivotal role of PAR chain length. Our data demonstrate for the first time that the affinity of the non-covalent PAR interactions with specific binding proteins (XPA, p53) can be very high (nanomolar range) and is dependent both on the PAR chain length and on the binding protein. Moreover, we developed an efficient protocol for the large-scale preparation of size-fractionated, biotinylated PAR and established several novel methods, particularly EMSA and SPR, to study the interaction of PAR and specific binding proteins as a function of PAR chain length. These new tools will be instrumental for the precise characterization of this non-covalent binding and for clarification of the signaling role of ADP-ribose polymers.

REFERENCES

1. Ame,J.C., Spenlehauer,C. and de Murcia,G. (2004) The PARP superfamily. *Bioessays*, **26**, 882 893.
2. D'Amours,D., Desnoyers,S., D'Silva,I. and Poirier,G.G. (1999) Poly(ADP ribosyl)ation reactions in the regulation of nuclear functions. *Biochem. J.*, **342**, 249 268.
3. Braun,S.A., Panzeter,P.L., Collinge,M.A. and Althaus,F.R. (1994) Endoglycosidic cleavage of branched polymers by poly(ADP ribose) glycohydrolase. *Eur. J. Biochem.*, **220**, 369 375.
4. Meyer,R.G., Meyer Ficca,M.L., Whatcott,C.J., Jacobson,E.L. and Jacobson,M.K. (2007) Two small enzyme isoforms mediate mammalian mitochondrial poly(ADP ribose) glycohydrolase (PARG) activity. *Exp. Cell Res.*, **313**, 2920 2936.
5. Mendoza Alvarez,H. and Alvarez Gonzalez,R. (2001) Regulation of p53 sequence specific DNA binding by covalent poly(ADP ribosyl)ation. *J. Biol. Chem.*, **276**, 36425 36430.
6. Thorslund,T., von Kobbe,C., Harrigan,J.A., Indig,F.E., Christiansen,M., Stevnsner,T. and Bohr,V.A. (2005) Cooperation of the Cockayne syndrome group B protein and poly(ADP ribose) polymerase 1 in the response to oxidative stress. *Mol. Cell. Biol.*, **25**, 7625 7636.
7. Adamietz,P. and Rudolph,A. (1984) ADP ribosylation of nuclear proteins in vivo. Identification of histone H2B as a major acceptor for mono and poly(ADP ribose) in dimethyl sulfate treated hepatoma AH 7974 cells. *J. Biol. Chem.*, **259**, 6841 6846.
8. Poirier,G.G., de Murcia,G., Jongstra Bilen,J., Niedergang,C. and Mandel,P. (1982) Poly(ADP ribosyl)ation of polynucleosomes causes relaxation of chromatin structure. *Proc. Natl Acad. Sci. USA*, **79**, 3423 3427.
9. Kameoka,M., Ota,K., Tetsuka,T., Tanaka,Y., Itaya,A., Okamoto,T. and Yoshihara,K. (2000) Evidence for regulation of NF kappaB by poly(ADP ribose) polymerase. *Biochem. J.*, **346**, 641 649.
10. Masson,M., Niedergang,C., Schreiber,V., Muller,S., Menissier de Murcia,J. and de Murcia,G. (1998) XRCC1 is specifically associated with poly(ADP ribose) polymerase and negatively regulates its activity following DNA damage. *Mol. Cell. Biol.*, **18**, 3563 3571.
11. Prasad,R., Lavrik,O.I., Kim,S.J., Kedar,P., Yang,X.P., Vande Berg,B.J. and Wilson,S.H. (2001) DNA polymerase beta mediated long patch base excision repair. Poly(ADP ribose)polymerase 1 stimulates strand displacement DNA synthesis. *J. Biol. Chem.*, **276**, 32411 32414.
12. Schreiber,V., Ame,J.C., Dolle,P., Schultz,I., Rinaldi,B., Fraulob,V., Menissier de Murcia,J. and de Murcia,G. (2002) Poly(ADP ribose) polymerase 2 (PARP 2) is required for efficient base excision DNA repair in association with PARP 1 and XRCC1. *J. Biol. Chem.*, **277**, 23028 23036.
13. Meyer,R., Muller,M., Beneke,S., Kupper,J.H. and Burkle,A. (2000) Negative regulation of alkylation induced sister chromatid exchange by poly(ADP ribose) polymerase 1 activity. *Int. J. Cancer*, **88**, 351 355.
14. Simbulan Rosenthal,C.M., Haddad,B.R., Rosenthal,D.S., Weaver,Z., Coleman,A., Luo,R., Young,H.M., Wang,Z.Q.,

Ried,T. *et al.* (1999) Chromosomal aberrations in PARP(/) mice: genome stabilization in immortalized cells by reintroduction of poly(ADP ribose) polymerase cDNA. *Proc. Natl Acad. Sci. USA*, **96**, 13191 13196.

15. Masutani,M., Nakagama,H. and Sugimura,T. (2005) Poly(ADP ribosyl)ation in relation to cancer and autoimmune disease. *Cell Mol. Life Sci.*, **62**, 769 783.

16. Burkle,A. (2005) Poly(ADP ribose). The most elaborate metabolite of NAD+. *FEBS J.*, **272**, 4576 4589.

17. Minaga,T. and Kun,E. (1983) Probable helical conformation of poly(ADP ribose). The effect of cations on spectral properties. *J. Biol. Chem.*, **258**, 5726 5730.

18. Alvarez Gonzalez,R. and Jacobson,M.K. (1987) Characterization of polymers of adenosine diphosphate ribose generated in vitro and in vivo. *Biochemistry*, **26**, 3218 3224.

19. Kiehlbauch,C.C., Aboul Ela,N., Jacobson,E.L., Ringer,D.P. and Jacobson,M.K. (1993) High resolution fractionation and charac terization of ADP ribose polymers. *Anal. Biochem.*, **208**, 26 34.

20. Pleschke,J.M., Kleczkowska,H.E., Strohm,M. and Althaus,F.R. (2000) Poly(ADP ribose) binds to specific domains in DNA damage checkpoint proteins. *J. Biol. Chem.*, **275**, 40974 40980.

21. Malanga,M., Pleschke,J.M., Kleczkowska,H.E. and Althaus,F.R. (1998) Poly(ADP ribose) binds to specific domains of p53 and alters its DNA binding functions. *J. Biol. Chem.*, **273**, 11839 11843.

22. El Khamisy,S.F., Masutani,M., Suzuki,H. and Caldecott,K.W. (2003) A requirement for PARP 1 for the assembly or stability of XRCC1 nuclear foci at sites of oxidative DNA damage. *Nucleic Acids Res.*, **31**, 5526 5533.

23. Okano,S., Lan,L., Caldecott,K.W., Mori,T. and Yasui,A. (2003) Spatial and temporal cellular responses to single strand breaks in human cells. *Mol. Cell. Biol.*, **23**, 3974 3981.

24. Malanga,M. and Althaus,F.R. (2004) Poly(ADP ribose) reactivates stalled DNA topoisomerase I and Induces DNA strand break resealing. *J. Biol. Chem.*, **279**, 5244 5248.

25. Haince,J.F., Kozlov,S., Dawson,V.L., Dawson,T.M., Hendzel,M.J., Lavin,M.F. and Poirier,G.G. (2007) Ataxia Telangiectasia Mutated (ATM) signaling network is modulated by a novel poly(ADP ribose) dependent pathway in the early response to DNA damaging Agents. *J. Biol. Chem.*, **282**, 16441 16453.

26. Chang,P., Jacobson,M.K. and Mitchison,T.J. (2004) Poly(ADP ribose) is required for spindle assembly and structure. *Nature*, **432**, 645 649.

27. Schreiber,V., Dantzer,F., Ame,J.C. and de Murcia,G. (2006) Poly(ADP ribose): novel functions for an old molecule. *Nat. Rev. Mol. Cell Biol.*, **7**, 517 528.

28. Panzeter,P.L., Realini,C.A. and Althaus,F.R. (1992) Noncovalent interactions of poly(adenosine diphosphate ribose) with histones. *Biochemistry*, **31**, 1379 1385.

29. Panzeter,P.L., Zweifel,B., Malanga,M., Waser,S.H., Richard,M. and Althaus,F.R. (1993) Targeting of histone tails by poly(ADP ribose). *J. Biol. Chem.*, **268**, 17662 17664.

30. Kawamitsu,H., Hoshino,H., Okada,H., Miwa,M., Momoi,H. and Sugimura,T. (1984) Monoclonal antibodies to poly(adenosine diphosphate ribose) recognize different structures. *Biochemistry*, **23**, 3771 3777.

31. Beneke,S., Alvarez Gonzalez,R. and Burkle,A. (2000) Comparative characterisation of poly(ADP ribose) polymerase 1 from two mammalian species with different life span. *Exp. Gerontol.*, **35**, 989 1002.

32. Chalkley,G.E., Knowles,P.P., Whitehead,P.C. and Coffer,A.I. (1994) Biochemical characterisation of purified human wild type p53 overexpressed in insect cells. *Eur. J. Biochem.*, **221**, 167 175.

33. Nuber,U., Schwarz,S.E. and Scheffner,M. (1998) The ubiquitin protein ligase E6 associated protein (E6 AP) serves as its own substrate. *Eur. J. Biochem.*, **254**, 643 649.

34. Jones,C.J. and Wood,R.D. (1993) Preferential binding of the xeroderma pigmentosum group A complementing protein to damaged DNA. *Biochemistry*, **32**, 12096 12104.

35. Missura,M., Buterin,T., Hindges,R., Hubscher,U., Kasparkova,J., Brabec,V. and Naegeli,H. (2001) Double check probing of DNA bending and unwinding by XPA RPA: an architectural function in DNA repair. *The EMBO J.*, **20**, 3554 3564.

36. Malanga,M., Bachmann,S., Panzeter,P.L., Zweifel,B. and Althaus,F.R. (1995) Poly(ADP ribose) quantification at the femtomole level in mammalian cells. *Anal. Biochem.*, **228**, 245 251.

37. Shah,G.M., Poirier,D., Duchaine,C., Brochu,G., Desnoyers,S., Lagueux,J., Verreault,A., Hoflack,J.C., Kirkland,J.B. *et al.* (1995) Methods for biochemical study of poly(ADP ribose) metabolism in vitro and in vivo. *Anal. Biochem.*, **227**, 1 13.

38. Panzeter,P.L. and Althaus,F.R. (1990) High resolution size analysis of ADP ribose polymers using modified DNA sequencing gels. *Nucleic Acids Res.*, **18**, 2194.

39. Cooper,M.A. (2003) Label free screening of bio molecular interac tions. *Anal. Bioanal. Chem.*, **377**, 834 842.

40. Karlsson,R., Katsamba,P.S., Nordin,H., Pol,E. and Myszka,D.G. (2006) Analyzing a kinetic titration series using affinity biosensors. *Anal. Biochem.*, **349**, 136 147.

41. Karlsson,R. and Falt,A. (1997) Experimental design for kinetic analysis of protein protein interactions with surface plasmon resonance biosensors. *J. Immunol. Methods*, **200**, 121 133.

42. Linnell,J., Mott,R., Field,S., Kwiatkowski,D.P., Ragoussis,J. and Udalova,I.A. (2004) Quantitative high throughput analysis of transcription factor binding specificities. *Nucleic Acids Res.*, **32**, e44.

43. Hainaut,P., Hall,A. and Milner,J. (1994) Analysis of p53 quaternary structure in relation to sequence specific DNA binding. *Oncogene*, **9**, 299 303.

44. Narendja,F.M. and Sauermann,G. (1994) The use of biotinylated poly(ADP ribose) for studies on poly(ADP ribose) protein interac tion. *Anal. Biochem.*, **220**, 415 419.

45. Cheung,A. and Zhang,J. (2000) A scintillation proximity assay for poly(ADP ribose) polymerase. *Anal. Biochem.*, **282**, 24 28.

46. Bondeson,K., Frostell Karlsson,A., Fagerstam,L. and Magnusson,G. (1993) Lactose repressor operator DNA interac tions: kinetic analysis by a surface plasmon resonance biosensor. *Anal. Biochem.*, **214**, 245 251.

47. Cleaver,J.E. (2005) Cancer in xeroderma pigmentosum and related disorders of DNA repair. *Nat. Rev. Cancer*, **5**, 564 573.

48. Kauppinen,T.M., Chan,W.Y., Suh,S.W., Wiggins,A.K., Huang,E.J. and Swanson,R.A. (2006) Direct phosphorylation and regulation of poly(ADP ribose) polymerase 1 by extracellular signal regulated kinases 1/2. *Proc. Natl Acad. Sci. USA*, **103**, 7136 7141.

49. Cohen Armon,M., Visochek,L., Rozensal,D., Kalal,A., Geistrikh,I., Klein,R., Bendetz Nezer,S., Yao,Z. and Seger,R. (2007) DNA independent PARP 1 activation by phosphorylated ERK2 increases Elk1 activity: a link to histone acetylation. *Mol. Cell*, **25**, 297 308.

50. Keil,C., Grobe,T. and Oei,S.L. (2006) MNNG induced cell death is controlled by interactions between PARP 1, poly(ADP ribose) glycohydrolase, and XRCC1. *J. Biol. Chem.*, **281**, 34394 34405.

51. Berger,F., Lau,C. and Ziegler,M. (2007) Regulation of poly(ADP ribose) polymerase 1 activity by the phosphorylation state of the nuclear NAD biosynthetic enzyme NMN adenylyl transferase 1. *Proc. Natl Acad. Sci. USA*, **104**, 3765 3770.

52. Andrabi,S.A., Kim,N.S., Yu,S.W., Wang,H., Koh,D.W., Sasaki,M., Klaus,J.A., Otsuka,T., Zhang,Z. *et al.* (2006) Poly(ADP ribose) (PAR) polymer is a death signal. *Proc. Natl Acad. Sci. USA*, **103**, 18308 18313.

53. Yu,S.W., Andrabi,S.A., Wang,H., Kim,N.S., Poirier,G.G., Dawson,T.M. and Dawson,V.L. (2006) Apoptosis inducing factor mediates poly(ADP ribose) (PAR) polymer induced cell death. *Proc. Natl Acad. Sci. USA*, **103**, 18314 18319.

54. Yu,S.W., Wang,H., Poitras,M.F., Coombs,C., Bowers,W.J., Federoff,H.J., Poirier,G.G., Dawson,T.M. and Dawson,V.L. (2002) Mediation of poly(ADP ribose) polymerase 1 dependent cell death by apoptosis inducing factor. *Science*, **297**, 259 263.